Journal of Engineering Mathematics **42:** 341–357, 2002.

Thin liquid films flowing over external aerodynamic surfaces

A.P. ROTHMAYER[1], B.D. MATHEIS[1] and S.N. TIMOSHIN[2]
[1]*Department of Aerospace Engineering and Engineering Mechanics, 1200 Howe Hall, Iowa State University. Ames, Iowa 50011, U.S.A.;* [2]*Department of Mathematics, University College London, Gower Street, London, WCIE 6BT, U.K.*

Received 24 October 2001; accepted in revised form 30 January 2002

Abstract. Boundary-layer theories are constructed to describe the evolution of interfacial waves on thin liquid films which are driven by an air boundary layer. The theories are focused on cases which are most relevant to aircraft icing. It is found that condensed-layer solutions with film inertia adequately describe the linear evolution of interfacial waves for thinner films, whereas a triple-deck pressure displacement interaction is required for thicker films. In all cases it is found that inertia must be retained within the film, even when the film is much more viscous than the air.

Key words: asymptotics, high Reynolds numbers, instability, liquid films

1. Introduction

The goal of this study is to identify boundary-layer structures that can be used to model efficiently surface-water processes for aircraft icing. Aircraft icing occurs when an aerodynamic surface such as a wing or tail-plane passes through a cloud of supercooled water droplets. Supercooled droplets are small water droplets suspended in the atmosphere whose temperature is below the freezing temperature of water. This is an unstable equilibrium state in a larger mass of water. When these droplets strike the aircraft surface they tend to freeze rapidly and form complex ice structures that can significantly impact the aerodynamics and performance of the aircraft (see Figure 1 and Gent *et al.* [1]). The droplet clouds are characterized by the mean size of the droplets called the Mean Volume Diameter or MVD and the Liquid Water Content or LWC. The dimensional LWC* is simply the total mass of water per unit volume contained in the droplet cloud. MVD's are typically small, on the order of $10-50$ microns, with the largest individual droplet diameters ranging up to a few hundred microns. LWC*'s are also typically small, about $0{\cdot}5$ g/m^3 and rarely exceeding $1-3$ g/m^3. When the droplets strike an aerodynamic surface at low temperature they can immediately freeze on impact producing a milky white ice called rime ice. If temperatures are closer to freezing, and airspeeds and LWC*'s are higher, then not all of the water freezes on impact and residual water can be left on the surface. It is generally believed that this residual water can act to redistribute water mass along the surface (see Messinger [2] and Myers [3]). The form of the residual water can vary depending on local conditions and it is generally expected that films, beads, rivulets, and patches of water can all be present on the airfoil surface at one time or another. There is clear experimental evidence that water films do exist in icing conditions sufficiently close to the stagnation point (Olsen and Walker [4]).

In this study we will examine one of these cases, namely thin water films that are generated by low LWC* droplet impacts on an external aerodynamic surface. The films created on the

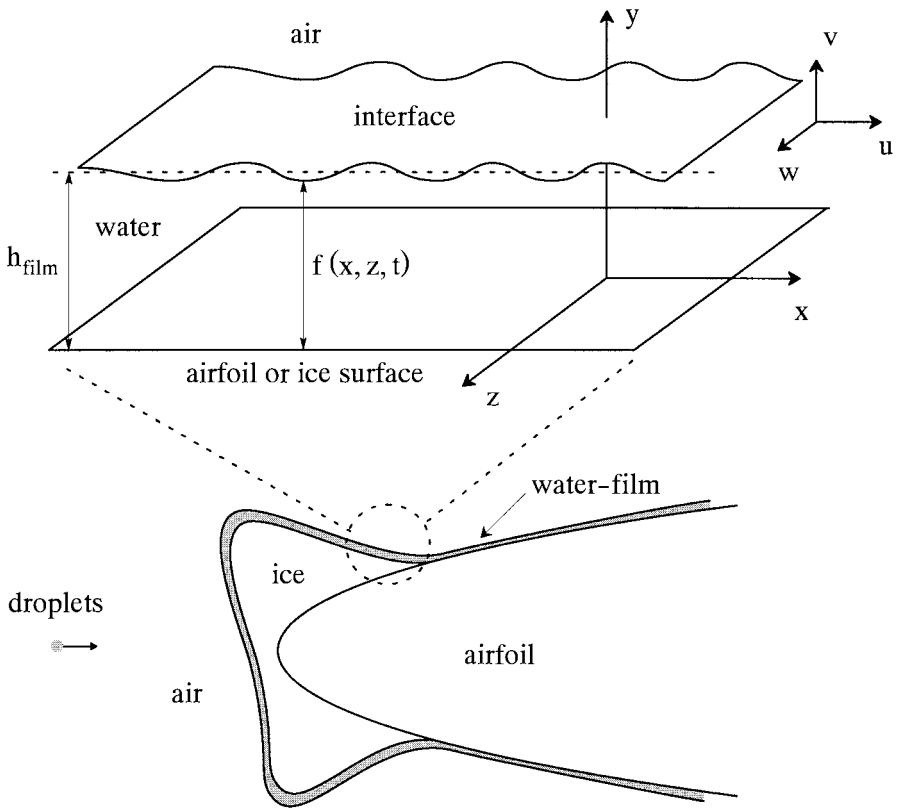

Figure 1. Geometry of the airfoil, accreted ice and water film.

surface are driven info motion by the air Prandtl boundary layer and the nature of the flow within the film is dependent upon the details of the interaction between the film and the air boundary layer. The primary goal of this study is to determine scaling laws for these films and to assess when simple lubrication models can be used within the film. In addition, we seek to identify limits on the validity of the scaling laws when changing parameters such as film thickness and the surface tension of the film. Of particular concern is the identification of scaling laws which are applicable to aircraft icing. This requirement places restrictions on the types of films that should be considered, and, in particular, limits our discussion to situations where the liquid film density and viscosity are much larger than those of air.

In the aerodynamic application considered here, the typical *Reynolds* number in the flow is large and the use of a high-Reynolds-number asymptotic theory seems appropriate. The flow in a boundary layer on a film-coated wall was considered by Timoshin [5] for the regime of complete viscous-inviscid interaction between near-wall viscous layers and the flow outside the boundary layer. All of the boundary-layer structures considered in this study may be viewed as a subset of this general problem. In that study, the film flow was assumed to be confined to the viscous sublayer of the triple-deck, and was found to provide the setting for a simultaneous description of both linear Tollmien-Schlichting and interfacial instabilities as well as nonlinear wave evolution and flow separation. A related triple-deck study was conducted by Tsao *et al.* [6] using a strong lubrication approximation within the film, to be discussed later, with application to airfoil leading edges.

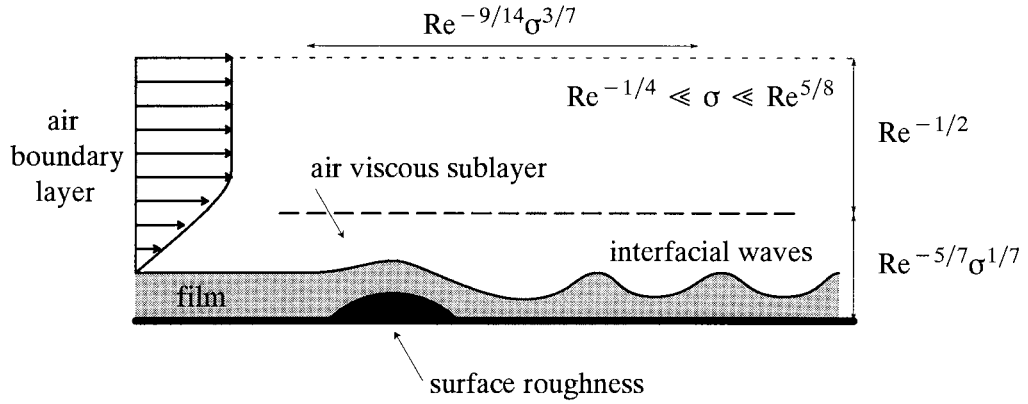

Figure 2. Condensed-layer scales.

In certain ranges of the relative densities and viscosities of the two fluids, the multiple instability modes contained within the triple-deck interact in a complicated fashion (with both direct mode crossing and resonant interactions possible under the right conditions, see Bowles *et al.* [7] and Timoshin and Hooper [8]). It should be noted, however, that the spectrum of Tollmien-Schlichting/interfacial-wave interactions proves to be more limited for the central problem considered in this paper, namely that of air-driven liquid films applicable to aircraft icing, and one of our aims here is to verify this conclusion in computations which extend the results of earlier studies. We find, in particular, that for all realistic choices of the scaled film thickness and surface tension, the Tollmien-Schlichting modes remain essentially unaffected by the film evolution in the linear approximation, mainly because of the large density difference between water and air. This property was noted earlier in Pelekasis and Tsamopoulos [9] who also found that the interfacial instability alone may lead to absolute instability in the flow (see also Rothmayer and Tsao [10]).

It should be noted that it is not always obvious to what extent the conclusions drawn from a high-Reynolds-number theory can be translated to flow properties at large but finite Reynolds number. For example, it appears that the triple-deck structure discussed below does not reproduce a mode intersection described in Ozgen *et al.* [11] for a particular finite Reynolds number. A more systematic study of both asymptotic and finite Reynolds flows should help fill the existing gaps in our understanding of two-fluid boundary layers and related flows. In this paper, the focus will remain on the asymptotic analysis and its implications for external aerodynamics.

2. Short-scaled nonlinear interactions – The condensed layer

The generation of air-driven surface waves on a film requires a feedback mechanism between the air and water. It turns out that such a mechanism is present on short scales for near-wall viscous layers for which the displacement of the viscous sublayer is zero, and these are called *condensed layers* (see Bogolepov and Neiland [12, 13], Smith *et al.* [14], and Rothmayer and Smith [15]). It is known that the airflow within such layers responds to wall distortions (film waves in our case) of length Δ and height $Re^{-1/2}\Delta^{1/3}$ and produces a pressure reaction of order $\Delta^{2/3}$ (see Rothmayer and Smith [15]). The dominant surface film waves are found to occur when the destabilizing effect of this air forcing (either pressure or shear) is counterbalanced

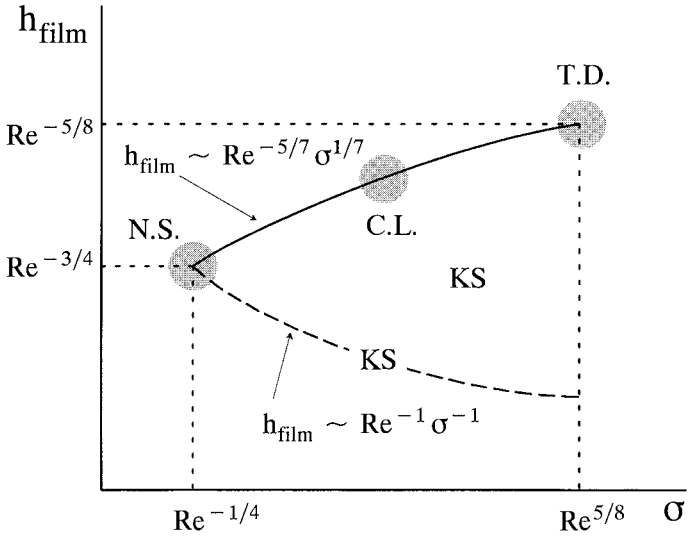

Figure 3. Surface tension and film-thickness parameter space, showing the various structures considered in this study. N.S. = Navier-Stokes region; C.L. = condensed layer; T.D. = triple-deck; KS = regions known to be controlled by modified Kuramoto-Sivashinsky equations (see Rothmayer and Tsao [10])

by the stabilizing effect of surface tension. For example, a pressure response to the interfacial wave distortion is balanced by surface tension when:

$$p_{\text{water}} - p_{\text{air}} \sim \text{Re}^{-1}\sigma \frac{\partial^2 f_{\text{water}}}{\partial x^2}, \tag{1}$$

where p is pressure, x is streamwise distance along the airfoil/ice and f is the air-water interface height (see Figure 1). The non-dimensional parameters used in the condensed layer are the Reynolds number $\text{Re} = \rho_\infty V_\infty L/\mu_\infty \gg 1$, the non-dimensional surface tension $\sigma = \sigma^*/(V_\infty \mu_\infty)$ (which is related to Weber number by $\text{We} = \text{Re}\sigma^{-1}$), the water-to-air viscosity ratio $\text{M} = \mu^*_{\text{water}}/\mu_\infty \gg 1$ and the air-to-water density ratio $D_{\text{aw}} = \rho_\infty/\rho^*_{\text{water}} \ll 1$. The variables here have their usual meanings, $(\,)^*$ denotes a dimensional value and ∞ denotes freestream conditions. We also assume in this study that the air is evaluated at constant temperature and low Mach number and is effectively incompressible. More general cases are considered in Rothmayer and Tsao [10].

Substituting the condensed-layer estimates for the various terms in (1) and solving for the streamwise length-scale we have

$$\Delta^{2/3} \sim \text{Re}^{-1}\sigma \frac{\text{Re}^{-1/2}\Delta^{1/3}}{\Delta^2} \Rightarrow \Delta \sim \text{Re}^{-9/14}\sigma^{3/7}. \tag{2}$$

The film thickness is on the order of the air viscous-sublayer thickness and is (see Figures 2 and 3)

$$h_{\text{film}} \sim \text{Re}^{-1/2}\Delta^{1/3} \sim \text{Re}^{-5/7}\sigma^{1/7}. \tag{3}$$

Formally, we assume that the air-water interface is located at $f \sim \text{Re}^{-5/7}\sigma^{1/7}F$ and the undisturbed film thickness is $F = h$. This structure will be termed a condensed layer and its location in a surface-tension and film-thickness parameter space is shown in Figure 3. The streamwise length scale of condensed-layer interfacial waves, as given by (2), is close to the

boundary-layer thickness in length, due to the fact that σ is only a modestly large number. In addition, the air sublayer thickness for the condensed layers, and hence the film thickness, is a small fraction of the air boundary-layer thickness. Formally, Rothmayer and Tsao [10] assume the following expansions in the condensed layer:

$$(x, y, z) = (\mathrm{Re}^{-9/14}\sigma^{3/7}X, \mathrm{Re}^{-5/7}\sigma^{1/7}Y, \mathrm{Re}^{-9/14}\sigma^{3/7}Z).$$

The time scale is chosen to be the slowest one in the problem, which comes from the water-interface motion, and is

$$t = \mathrm{Re}^{-3/7}\sigma^{2/7}D_{\mathrm{aw}}^{-1/2}\mathcal{M}T. \tag{4}$$

In all of the condensed-layer structures to be discussed in this paper we will assume the following relation between the air/water density ratio and the air/water viscosity ratio:

$$M = \mathcal{M}D_{\mathrm{aw}}^{-1/2}.$$

In the context of our study, the justification for this equation is simply that this balance holds for water and air over a wide range of temperatures applicable to aircraft icing problems (with $\mathcal{M}$ typically lying between 2 and 4) and that the condensed-layer equations critically depend upon whether or not this particular balance is true. It may be shown that the time scale of (4) is faster than the time scale of the larger-scale film evolution which is driven by the air Prandtl boundary layer providing that $\sigma \ll \mathrm{Re}^{3/2}$. This condition is found to be true given the bounds on σ to be discussed in Section 3 (see Figure 3). The dependent variables in the air take on the standard form for a condensed-air sublayer but with the streamwise scaling of (2) (see Rothmayer and Smith [15])

$$(u, v, w) \sim (\mathrm{Re}^{-3/14}\sigma^{1/7}u, \mathrm{Re}^{-2/7}\sigma^{-1/7}v, \mathrm{Re}^{-3/14}\sigma^{1/7}w),$$
$$p \sim P_B + \mathrm{Re}^{-3/7}\sigma^{2/7}p,$$

where lower-case variables are used for air and upper-case variables for water. The equations in the air are then

$$u_X + v_Y + w_Z = 0,$$
$$uu_X + vu_Y + wu_Z = -p_X(X, Z, T) + u_{YY},$$
$$uw_X + vw_Y + ww_Z = -p_Z(X, Z, T) + w_{YY}.$$

The boundary conditions are given by

$$\begin{aligned} &u \to \lambda(Y - h) \quad \text{as} \quad Y \to \infty \\ &u(X, F, Z) = v(X, F, Z) = w(X, F, Z) = 0, \end{aligned} \tag{5}$$

where $\tau_w = \lambda\mathrm{Re}^{-1/2}$ is the wall shear stress of the undisturbed air boundary layer. The air equations are quasi-steady due to the fact that the time scale of the air-water interface is much slower than the natural air time scale. The water-dependent variables are determined from a direct pressure and shear-stress match with the air. The shear-stress match requires that the water velocities within the film be scaled down from the air velocities by a factor of the viscosity ratio between air and water, *i.e.* $M = \mathcal{M}D_{\mathrm{aw}}^{-1/2}$. This result is responsible for the no-slip air boundary conditions (5) emerging from the more general air-water velocity match to be discussed in Section 3. Formally, the dependent variables within the water film are:

$$(u, v, w) \sim (\mathrm{Re}^{-3/14}\sigma^{1/7}D_{\mathrm{aw}}^{1/2}\mathcal{M}^{-1}U, \mathrm{Re}^{-2/7}\sigma^{-1/7}D_{\mathrm{aw}}^{1/2}\mathcal{M}^{-1}V, \mathrm{Re}^{-3/14}\sigma^{1/7}D_{\mathrm{aw}}^{1/2}\mathcal{M}^{-1}W),$$

$$p \sim P_B + \mathrm{Re}^{-3/7}\sigma^{2/7}P.$$

The equations within the water film are

$$U_X + V_Y + W_Z = 0,$$

$$\mathcal{M}^{-2}[U_T + UU_X + VU_Y + WU_Z] = -P_X(X, Z, T) + U_{YY},$$

$$\mathcal{M}^{-2}[W_T + UW_X + VW_Y + WW_Z] = -P_Z(X, Z, T) + W_{YY},$$

with the no-slip boundary conditions (5) also holding at the bottom of the film (*i.e.* $Y = 0$). Note that, even though a large-viscosity-ratio approximation is used (*i.e.* $M \gg 1$), the large water-to-air inertia ($D_{\mathrm{aw}} \ll 1$) brings the viscous and convective terms into balance within the film. This balance is controlled by $\mathcal{M}$ and only depends on local temperature, *i.e.* it does not depend upon changes in Reynolds number or water surface tension. This will be termed a *weak lubrication approximation*. The remaining boundary conditions are all evaluated along the air-water interface at $Y = F(X, Z, T)$. The stress match on the air-water interface gives

$$U_Y(X, F, Z) = u_Y(X, F, Z), \qquad W_Y(X, F, Z) = w_Y(X, F, Z)$$

and

$$P(X, F, Z) = p(X, F, Z) + \mathcal{K}, \tag{6}$$

where the interface curvature is $\mathcal{K} = -[F_{XX} + F_{ZZ}]$. In addition, the kinematic condition for the interface is given by

$$V(X, F, Z) = F_T + U(X, F, Z)F_X + W(X, F, Z)F_Z \tag{7}$$

A simplified form of the above equations can be obtained by assuming that $\mathcal{M} \gg 1$. This will be termed a *strong lubrication approximation*, since in this limit inertia effects are absent from the film and a true lubrication equation is recovered for the film interface motion. When $\mathcal{M} \gg 1$ the equations within the film reduce to a Couette-Poiseuille system. The solution of these equations with no-slip boundary conditions at the solid surface under the film and the shear stress matching at the air-water interface gives:

$$U = \frac{\partial P}{\partial X}\frac{Y^2}{2} + Y\left[\tau_{WX} - \frac{\partial P}{\partial X}F\right], \qquad W = \frac{\partial P}{\partial Z}\frac{Y^2}{2} + Y\left[\tau_{WX} - \frac{\partial P}{\partial Z}F\right].$$

Substitution in the mass-conservation equation and integration gives an equation for V, which we will not write down here since it is fairly lengthy. All three velocities are then substituted in the kinematic condition (7). After some manipulation the following equation is obtained:

$$\frac{\partial F}{\partial T} + \frac{\partial}{\partial X}\left[\tau_{WX}\frac{F^2}{2} - \frac{\partial P}{\partial X}\frac{F^3}{3}\right] + \frac{\partial}{\partial Z}\left[\tau_{WZ}\frac{F^2}{2} - \frac{\partial P}{\partial Z}\frac{F^3}{3}\right] = 0,$$

where the water pressure is given by (6) and air shear stresses are $\tau_{WX} = \partial u/\partial Y(X, F, Z)$ and $\tau_{WZ} = \partial w/\partial Y(X, F, Z)$. We performed a linear stability analysis of the above system of equations using both the strong and weak lubrication approximations. The transformations $(X, Y) = (\lambda h^3\hat{X}, h\hat{Y})$, $T = h^2\mathcal{M}^{-2}\hat{T}$ and $(U, V, P) = \mathcal{M}^2(\lambda h\hat{U}, h^{-1}\hat{V}, \lambda^2 h^2\hat{P})$ are used to partially remove the parameters appearing in the above equations. The resulting equations in the water film for the weak lubrication approximation are controlled by the following two parameters

$$\Sigma = \frac{1}{\lambda^4 h^7}, \qquad \Lambda = \mathcal{M}^2. \tag{8}$$

In all of the linear stability analyses presented in this study, it is assumed that the surface underlying the water is flat and that the linear solution takes the normal mode form

$$F = h + \epsilon \overline{f} \exp(\sigma \hat{T} + \mathrm{i}\alpha \hat{X} + \mathrm{i}\beta \hat{Z}),$$

$$(u, v, w, p) = (\lambda \hat{Y}, 0, 0, 0) + \epsilon(\overline{u}, \overline{v}, \overline{w}, \overline{p}) \exp(\sigma \hat{T} + \mathrm{i}\alpha \hat{X} + \mathrm{i}\beta \hat{Z}),$$

where $h = \lambda = 1$ for the transformed problem and

$$\sigma = \sigma_R + i\sigma_I, \qquad \sigma_R > 0 \Rightarrow \text{ unstable}.$$

The above equations are substituted in the weak lubrication condensed-layer equations and the resulting linear system for the transformed problem is

$$\mathrm{i}\alpha \overline{u} + \overline{v}_{\hat{Y}} = 0, \qquad \sigma \overline{u} + \frac{\hat{Y}}{\Lambda} \mathrm{i}\alpha \overline{u} + \frac{1}{\Lambda} \overline{v} = -\mathrm{i}\alpha \overline{p} + \overline{u}_{\hat{Y}\hat{Y}},$$

with the boundary conditions along the air water interface given by

$$\Lambda \left(\overline{u}_{\hat{Y}}\right)_{\text{water}} = \left(\overline{u}_{\hat{Y}}\right)_{\text{air}}, \qquad v = \left(\sigma + \frac{\mathrm{i}\alpha}{\Lambda}\right) \overline{f}.$$

The air is governed by the steady-state linearized condensed-layer equations and these are solved in the standard fashion (see Smith [16], for example). The linear problem for the strong lubrication problem simplifies considerably. Here, the water film reduces to a Couette-Poiseuille system, which admits a simple solution. In fact, the following exact solution in un-transformed variables may be found for the growth rate:

$$h^2 \sigma_R = -\frac{\sqrt{3}}{2} \left[\lambda h^3 \frac{2\pi}{\lambda_X}\right]^{5/3} \mathrm{Ai}'(0) + \frac{3}{4} \mathrm{Ai}(0) \left[\lambda h^3 \frac{2\pi}{\lambda_X}\right]^{4/3} - \frac{16\pi^4 h^5}{3} \left[\lambda_X^{-2} + \lambda_Z^{-2}\right]^2, \tag{9}$$

where $\mathrm{Ai}(0) = 0{\cdot}35502$, $\mathrm{Ai}'(0) = -0{\cdot}25881$, $\alpha = 2\pi/\lambda_X$ and $\beta = 2\pi/\lambda_Z$. A typical growth rate for this instability is shown in Figure 4, both with and without surface tension. Surface tension acts to stabilize the waves at short wavelength. Note that the maximum growth rate occurs on these scales and is close to the neutral point. This instability is also found to obey a 'Squires Theorem', in the sense that instabilities with the largest growth rates are found to be the two-dimensional ones, *i.e.* $\beta = 0$ (see Rothmayer and Tsao [10]). A detailed examination of the eigenrelation (9) for $h \to 0$ and $h \to \infty$ reveals that all of the pressure forcing drops from the dispersion relation at leading order in the limit of small film thickness. At large film thickness all of the shear forcing drops from the leading-order dispersion relation (see Rothmayer and Tsao [10]).

Computations for the weak-lubrication approximation, (see Matheis [17]) shown in Figure 5 reveal that the role of inertia can be neglected for thin films, *i.e.* large Σ in this figure, see (8). However, for sufficiently thick films inertia plays a substantial role in determining the characteristrics of the waves (maximum growth rate in this case). Remembering that $\Sigma \sim O(h^{-7})$, we see that Figure 5 reveals that in all cases the film thickness only needs to be moderately large in condensed-layer variables in order for inertia to become important, a result that is consistent with the predictions of Rothmayer and Tsao [10]. The nonlinear interfacial waves emerging from the condensed-layer problem for the strong lubrication approximation

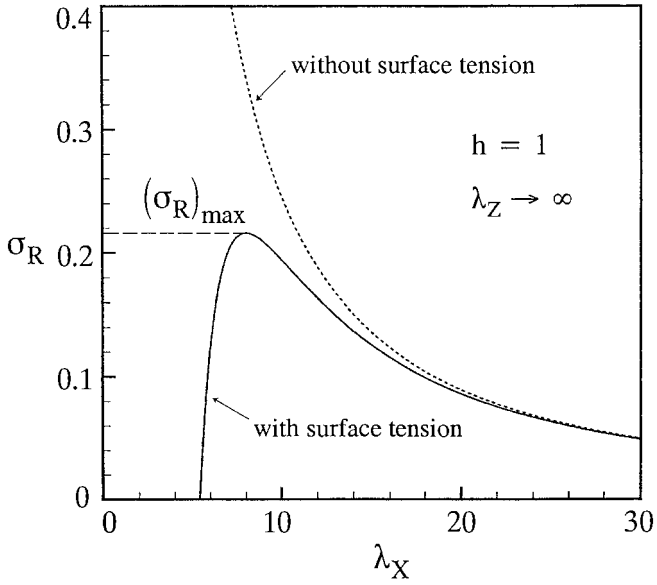

Figure 4. Instability growth rate for a typical linearly unstable solution in the condensed layer, with and without surface tension.

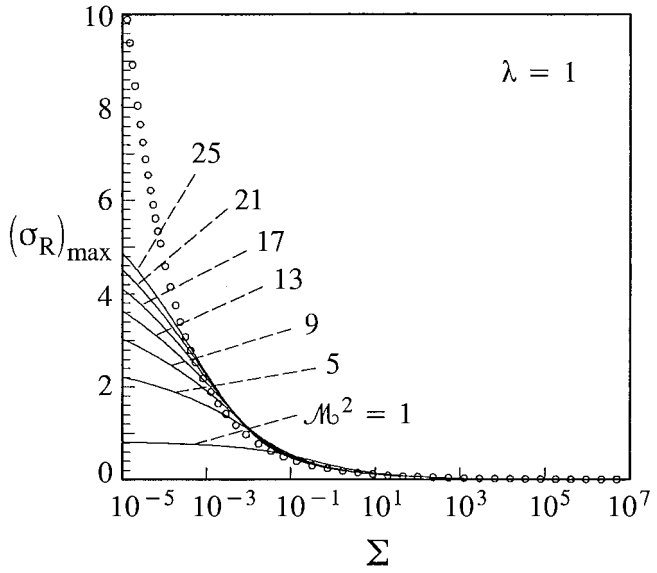

Figure 5. Maximum growth rate for typical condensed-layer interfacial waves using the weak-lubrication approximation. The ∘'s are the values of maximum growth rate for the strong-lubrication approximation.

are shown in Figure 6 (see Matheis [17]). Here, the linear waves at early time gradually evolve into regular nonlinear traveling waves at later time. As may be clearly seen from the streamline pattern in the air above the interfacial wave, the air solution at later time is separated for this particular case.

To summarize, the importance of the condensed layer is that it is the first film thickness for which inertia effects become important within the film. It is also the film thickness where the interfacial waves cross over from being shear-driven to being pressure-driven. From the

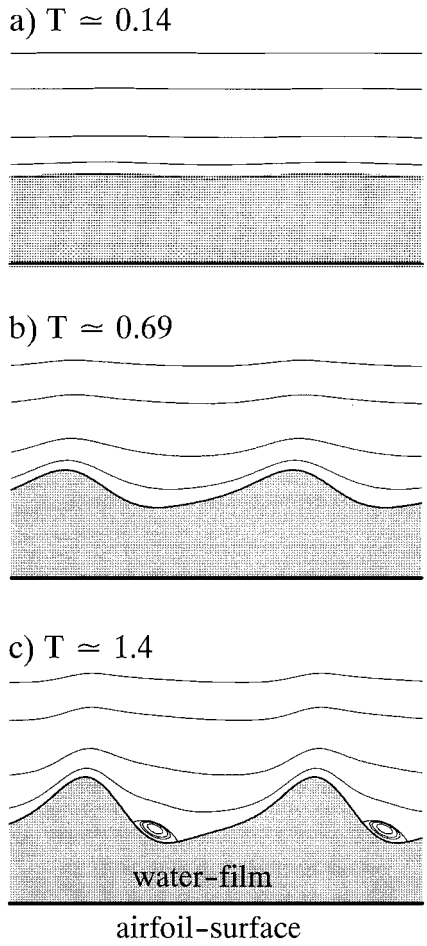

Figure 6. Typical nonlinear condensed-layer solution computed using the strong lubrication approximation, showing the initial low-amplitude wave and the final nonlinear traveling wave with separation in the air flow (the contours above the interfacial waves are the instantaneous air streamlines). Note that horizontal and vertical lengths are not plotted on the same scale.

point of view of engineering applications, it must be stressed that a lubrication approximation can only be used to describe the film motion when the film thickness is much less than the condensed-layer value of (3).

3. The role of surface tension

The streamwise scale of the condensed layer is controlled by surface tension. For water films, the non-dimensionalized value of the surface tension, σ, is a modestly large number, typically in the range of about 40 to 80. Here, we will address the question of how much the surface tension can change before affecting the condensed-layer structure. In practice this change is accomplished by natural changes in flow conditions, by deliberately adding surfactants to the water in controlled experiments or by inadvertently changing surface tension using die markers, de-icing fluids or other contaminants.

3.1. Large surface tension – The triple-deck emerging from the condensed layer

As the surface tension of the film increases, the wavelengths of the interfacial waves become longer (see (2) and Figures 2 and 3). Since the water film reacts only to the air sublayer, this means that the interfacial waves are insensitive to other secondary structures that occur in the various condensed layers approaching the triple-deck. Therefore, the condensed-layer structure fails when the streamwise wavelength increases to the scale of the triple-deck (*i.e.* $\mathrm{Re}^{-3/8}$), and this happens when $\sigma \sim O(\mathrm{Re}^{5/8})$. Formally, the triple-deck film thickness and surface tension are given by

$$\sigma = \mathrm{Re}^{5/8}\lambda^{-5/4}\Sigma, \qquad h_{\mathrm{film}} = \mathrm{Re}^{-5/8}\lambda^{-3/4}h$$

due to (1) and (10) through (13). Focusing on the two-dimensional problem, in both the air and water, we observe that the spatial coordinates and time in the triple-deck are

$$(x, y, t) = (\mathrm{Re}^{-3/8}\lambda^{-5/4}X, \mathrm{Re}^{-5/8}\lambda^{-3/4}Y, \mathrm{Re}^{-1/4}\lambda^{-3/2}D_{\mathrm{aw}}^{-1/2}\mathcal{M}T). \tag{10}$$

The dependent variables in the air are

$$(u, v) \sim (\mathrm{Re}^{-1/8}\lambda^{1/4}u, \mathrm{Re}^{-3/8}\lambda^{3/4}v), \qquad p \sim P_B + \mathrm{Re}^{-1/4}\lambda^{1/2}p, \tag{11}$$

whereas the dependent variables in the water are

$$(u, v) \sim (\mathrm{Re}^{-1/8}\lambda^{1/4}D_{\mathrm{aw}}^{1/2}\mathcal{M}^{-1}U, \mathrm{Re}^{-3/8}\lambda^{3/4}D_{\mathrm{aw}}^{1/2}\mathcal{M}^{-1}V), \tag{12}$$

$$p \sim P_B + \mathrm{Re}^{-1/4}\lambda^{1/2}P. \tag{13}$$

Notice that the large water-to-air viscosity ratio again produces small velocities within the water, *i.e.* in order to preserve the shear-stress match at the air-water interface, the water velocities are scaled down by a factor of $M^{-1} = D_{\mathrm{aw}}^{1/2}\mathcal{M}^{-1}$. The governing equations in the air then become:

$$u_X + v_Y = 0,$$
$$uu_X + vu_Y = -p_X(X, T) + u_{YY},$$

with the boundary conditions $u(X, F, T) = v(X, F, T) = 0$ and $u \to Y - h + A$ as $Y \to \infty$. The no-slip conditions applied to the air at the air-water interface are again a direct consequence of the slow velocities within the water film. The pressure displacement relation in the triple-deck is known to be

$$p(X, T) = \frac{U_e^2}{\pi}\int_{-\infty}^{\infty}\frac{A_\xi\,\mathrm{d}\xi}{X - \xi}, \tag{14}$$

where U_e is the inviscid slip velocity at the edge of the main air boundary layer. The governing equations within the water film are found to be

$$U_X + V_Y = 0,$$
$$\mathcal{M}^{-2}(U_T + UU_X + VU_Y) = -P_X(X, T) + U_{YY},$$

3.2. LARGE SURFACE TENSION – THE FULL TRIPLE-DECK FOR FLUID-FLUID INTERACTIONS

Our aim in this section is to make direct comparisons between the linear stability properties derived from the full triple-deck problem and those calculated for a two-fluid flow with a number of the limit regimes discussed earlier in this work and elsewhere. The full triple-deck assumes that M and D_{aw} are $O(1)$. As a result, the expansions (10) through (13) remain essentially unchanged and the velocities in the air and water are now of the same order of magnitude *i.e.* D_{aw} is finite in Equation (12)). The full triple-deck equations are those given above, but now with full unsteady boundary-layer equations in both the air and water, respectively:

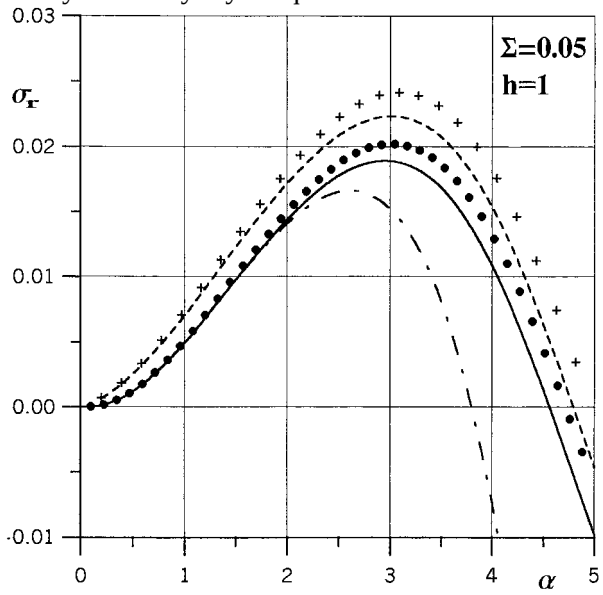

Figure 7. Comparison between full triple-deck solutions (solid line) and solutions obtained using various approximate models, for the growth-rate as a function of the wavenumber. Dashed lines – CTD model; dot-dashes – TDSL model; crosses – CL model; circles – TDWL model. The water/air density ratio is 1000, the air/water kinematic viscosity ratio is taken to be 14·9. The values for scaled surface tension and film thickness are indicated in the figure.

with no-slip boundary conditions applied at the bottom of the film and the following boundary conditions applied at the air-water interface $Y = F(X, T) : P = p - \Sigma F_{XX}, U_Y = u_y$ and $V = F_T + UF_X$. The above equations are a high-viscosity ratio, low-density ratio limit of the more general trip-deck problem studied by Timoshin [5], that we will term the *triple-deck with weak lubrication* or TDWL. Effectively, the triple-deck problem which limits to the condensed layer at short wavelengths is the full triple-deck interaction to be discussed next but with a quasi-steady approximation within the airflow and no-slip boundary conditions applied to the air at the air-water interface.

$$u_T + uu_X + vu_Y = -p_X + u_{YY},$$
$$U_T + UU_X + VU_Y = -D_{aw}P_X + MD_{aw}U_{YY}.$$

The boundary condition in the farfield of the triple-deck is again $u \to Y + A - h$ as $Y \to \infty$. A no-slip condition for the water flow is assumed at the bottom of the water film, *i.e.* at $Y = 0$.

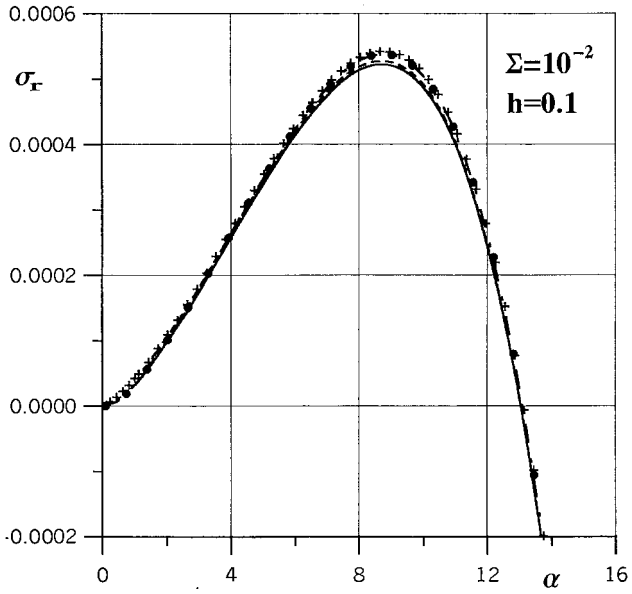

Figure 8. This shows the effect of decreasing surface tension on interfacial instability in the case of a relatively small fixed film thickness.

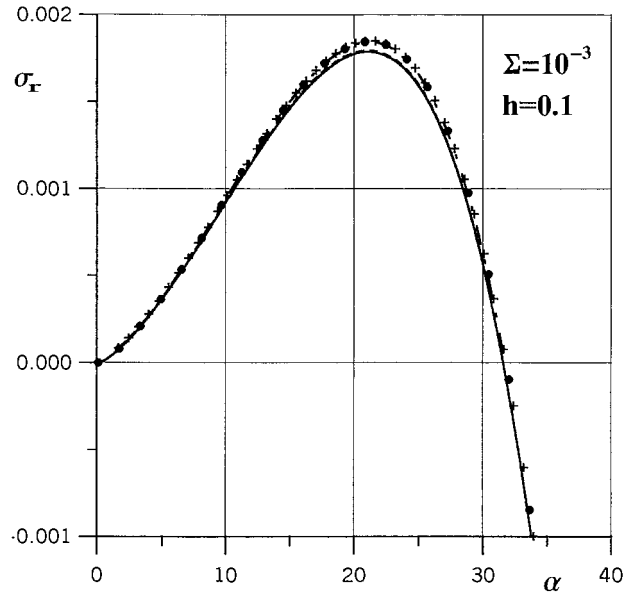

Figure 9. The comparison between full triple-deck and approximate models improves when surface tension decreases and the wavenumber range of most unstable modes broadens??

In addition, the pressure-displacement relation (14) holds for the air flow above the interface. The air-water interface conditions are applied at the air-water boundary $Y = F(X, T)$, where again $f - \mathrm{Re}^{-5/8}\lambda^{-3/4}F$, and include a full velocity match (with kinematic condition), a result which is absent in the models discussed above due to the assumed large velocity difference between air and water:

$$u = U, \qquad v = V = F_T + uF_X.$$

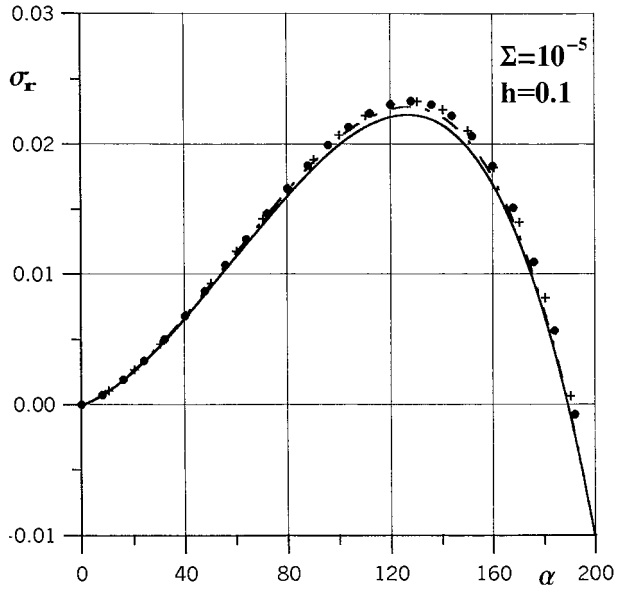

Figure 10. The trend observed in Figures 8 and 9 continues when the scales surface tension decreases further. No further qualitative changes in the behaviour of approximations to the triple-deck solutions seem to occur when the scaled surface tension falls below 0·01–0·001.

The interfacial stress match is essentially the same as that given previously, namely $P = p - \Sigma F_{XX}$ and $u_Y = MU_Y$. Again, $\sigma = \mathrm{Re}^{5/8}\lambda^{-5/4}\Sigma$ and $h_{\mathrm{film}} = \mathrm{Re}^{-5/8}\lambda^{-3/4}h$. It should be noted that for a typical icing wind-tunnel experiment, the surface tension of water is about $\sigma^* = 75{\cdot}6$ dynes/cm $= 0{\cdot}0756$ kg/s^2, the air viscosity at freezing is $\mu_\infty = 1{\cdot}708 \times 10^{-5}$ kg/(ms), the air speed is on the order of 100 m/s and, for example, the water film is generally believed to be about 20 microns thick on the leading edge of a 1 meter chord airfoil (with a Reynolds number on the order of 10^6). If we assume a representative value of the Prandtl-boundary-layer skin friction of $\lambda = 1$ (realizing that λ can vary from this value) then the triple-deck surface tension and film thickness are found to be about $\Sigma = 8 \times 10^{-3}$ and $h = 0{\cdot}1$, respectively. It is to be expected that the actual values can routinely vary from these nominal values by a factor of 2 or 3 and perhaps by as much as a factor of 10.

In the above estimate, increases in velocity will tend to lower σ (in proportion to V_∞^{-1}) and increase Re, hence lowering Σ. Larger values of Σ will only occur for very low velocities and Reynolds numbers, The triple-deck film thickness increases in proportion to the physical film thickness, so a film of 200 microns would give a triple-deck $h = 1{\cdot}0$ if the same flow conditions are assumed. An increase of Re by a factor of 10 will increase h by a factor of 4·2. Decreasing wall shear, such as when approaching a stagnation point, will tend to decrease h for fixed physical film thickness, thereby tending back towards condensed-layer properties (though one expects a breakdown and an emergence of Navier-Stokes properties sufficiently close to the stagnation point). The shear may reasonably be expected to increase to maximum values in the range of 2 or 3, which would increase h by a factor of 1·7–2·3. The most likely places where the triple-deck will become important is in high-shear regions at high Reynolds numbers for thicker films. For example, at a physical film thickness of 20 microns a maximum triple-deck h of 1·0 is to be expected. It is the authors' opinion that the triple-deck film thicknesses are realistic and can be encountered in practice, as are film thicknesses for which the condensed layer is valid. The exact situations for which each model is accurate, or

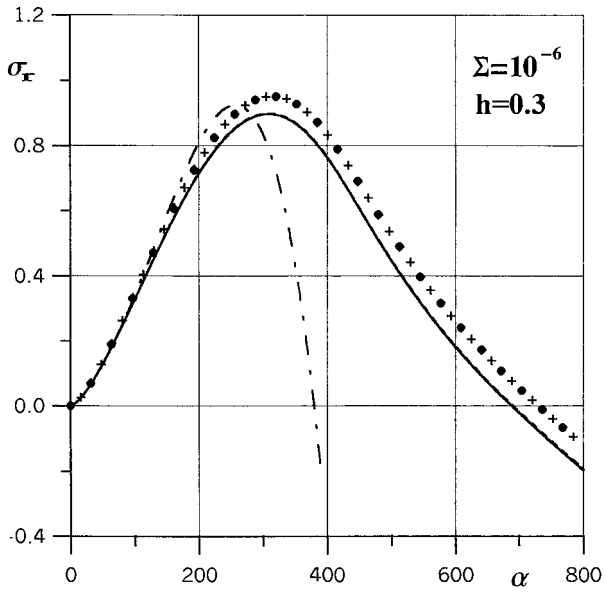

Figure 11. The results from C.L. (crosses) and TDWL (circles) models are almost identical. This indicates that the effects of viscous-inviscid interaction are not important at such large wavenumber scales.

is needed, depends upon the details of the flow solution and that issue is beyond the scope of the present study.

In the undisturbed state $u = Y - h + h/M, U = Y/M$ and $v = V = p = P = A = 0$, so that the flow is uni-directional along the flat interface with $F = h$. A small disturbance superimposed on the base flow and taken in the form $p = \exp(\sigma T + \mathrm{i}\alpha X)\overline{p}$ and $F = h + \exp(\sigma T + \mathrm{i}\alpha X)\overline{F}$ (and similar for all other functions) leads to the following eigenvalue problem (see Timoshin [5] for more detail)

$$[\mathrm{i}\alpha(Y - h + h/M) + \sigma]\overline{u}(Y) + \overline{v}(Y) = -\mathrm{i}\alpha\overline{p} + u''(Y),$$

$$\mathrm{i}\alpha\overline{u}(Y) + \overline{v}'(Y) = 0, \quad Y \geq h,$$

$$[\mathrm{i}\alpha Y/M + \sigma]\overline{U}(Y) + \overline{V}(Y)/M = -\mathrm{i}\alpha D_{aw}\overline{P} + MD_{aw}\overline{U}''(Y),$$

$$\mathrm{i}\alpha\overline{U}(Y) + \overline{V}'(Y) = 0, \quad 0 \leq Y \leq h,$$

$$\overline{u}(\infty) = \overline{A}, \qquad \overline{p} = |\alpha|\overline{A}, \qquad \overline{p} - \overline{P} = -\Sigma\alpha^2\overline{F}$$

$$\overline{U}(0) = \overline{V}(0) = 0, \qquad \overline{u}'(h) = M\overline{U}'(h),$$

$$\overline{u}(h) + \left(1 - \frac{1}{M}\right)\overline{F} = \overline{U}(h), \qquad \overline{v}(h) = \overline{V}(h) = [\mathrm{i}\alpha h/M + \sigma]\overline{F}.$$

In general, the linearized triple-deck formulation admits two classes of growing modes corresponding to either Tollmien-Schlichting or interfacial instabilities. In certain ranges of the viscosity and density ratios (M and D_{aw}) and especially for particular film thicknesses, the modes can coalesce and form a complex pattern of merged instabilities as shown by Timoshin [5] and Timoshin and Hooper [8]. However, the additional calculations performed in this study for the particular density and viscosity parameters corresponding to the air-water system show, in agreement with conclusions in Pelekasis and Tsamopoulos [9], that with realistic choices

of the film thickness h and the surface tension coefficient Σ the two instabilities are distinct and, more-over, the Tollmien-Schlichting instability growth rates are practically independent of the flow in the water film. Linear resonances of the type described in Bowles *et al.* [7] also do not appear in the air-water flow. We will focus, therefore, on the interfacial modes whose behavior proves to be highly sensitive to variations in film thickness and surface tension.

In what follows we will compare the properties of the interfacial triple-deck modes with the results derived for four limit forms of the high-Reynolds-number flow, all derived using the assumption of high viscosity of the fluid film. A limit form valid for sufficiently long waves and governed by a lubrication equation in the film and quasi-steady flow in the air was derived in Timoshin [5], see Section 5.2 therein, and Tsao *et al.* [6]. This limit form will be referred to as the *triple-deck with strong lubrication* or TDSL model. We will find, however, that this limit does not correctly describe the behavior of short-wave instabilities for which the *condensed layer*, or CL, equations may be more appropriate, and we will verify this assertion below. Also for the purpose of additional testing of the validity of condensed-layer equations we will include the results for a short-wave approximation of the triple-deck equation obtained by replacing the pressure-displacement interaction with the condensed-flow condition, $\overline{A} = 0$ all the other equations and boundary conditions remaining the same. This will be termed the *condensed triple-deck* or CTD. The model discussed at the start of Section 3 will be termed the *triple-deck with weak lubrication* or TDWL.

Solutions are presented for the growth rate σ_R as a function of the wavenumber, $\alpha = 2\pi/\lambda_X$, for a number of combinations of the parameters h and Σ. As shown in Figure 7, neither of the approximate systems can completely reproduce the full triple-deck growth-rate distribution in a flow with a sufficiently thick film and high surface tension. The TDSL model (dot-dashed line) shows reasonable agreement with the triple-deck solution in the long-wave range but fails at order-one wavenumbers. The condensed triple-deck or CTD (dashes) and condensed layer or CL (crosses) models reproduce qualitative trends of the triple-deck but give a considerable over-estimation of the growth rate over the entire wavenumber range. Clearly, the reason for this is the pressure-displacement interaction omitted in those two models. Also shown in Figure 7 (circles) is the improvement on the condensed-layer model when the pressure-displacement law $\overline{p} = |\alpha|\overline{A}$ is reintroduced back into the air-flow equations. This is the triple-deck with weak lubrication, or TDWL, discussed at the beginning of Section 3. In this figure, the new TDWL model does a pretty good job in reproducing the correct triple-deck behavior even at the larger film thicknesses, with a maximum error that is under 10%. It should be noted that the wavelength of maximum growth rate is in much better agreement between the different models than is the magnitude of the growth rate and the location of the neutral-stability points.

Waves on thinner films are better described by the approximations to the triple-deck model as is clear from Figure 8–10, and this is particularly true for the regimes with low surface tension when the maximum instability is pushed towards shorter wavelengths. The difference between full triple-deck and the condensed triple-deck or CTD solutions is practically negligible in Figure 10, and there is a favorable agreement between these two and the condensed layer and triple-deck with strong lubrication models also.

The behavior of the approximations to the full triple-deck models is most dramatic in the intermediate range of film thickness with small surface tension. Figure 11 shows that the triple-deck with strong lubrication solution fails completely for about 50 per cent of the unstable range. However, there is excellent agreement between the full triple-deck and condensed triple-deck solutions. The condensed-layer model also follows the trends of the full triple-

deck solution, with a slight overestimation of the maximum growth rate and the position of the upper branch neutral point.

Overall, our comparisons indicate that condensed-layer approximation can be used for the interfacial mode calculations with fair degree of confidence, provided that the film thickness remains smaller than the viscous-sublayer thickness for the conventional triple-deck and provided that the surface tension is sufficiently weak, so that the maximum instability does occur on wavelengths that are shorter than the triple-deck length scale. A way to extend the condensed-layer model into ranges of longer waves is to include the pressure-displacement interaction in the air flow of the condensed layer. The triple-deck with strong lubrication approximation only holds for thin films and high surface tension, whereas the triple-deck with weak lubrication model works reasonably well as long as the maximum instability takes place at the scaled wavenumber values of order 20, irrespective of the film thickness.

4. Conclusions

It is the contention of this study that surface-water films of the type encountered in aircraft icing applications can adequately be described by a lubrication approximation, until the film thickness has reached the critical thickness of the condensed layer or triple-deck. When this critical thickness is encountered, inertia becomes important within the film and interfacial waves begin to affect mass transport within the film (see Rothmayer and Tsao [10] for a discussion of this second issue). As the film thickness increases through the critical thickness, the interfacial waves change from being shear-driven to being pressure-driven. Since the condensed-layer interfacial waves are only affected by the near-wall airflow, the condensed layer is bounded by the triple-deck at large surface tension and by a near-wall Navier-Stokes region at small surface tension, *i.e.* by $\mathrm{Re}^{-1/4} \ll \sigma \ll \mathrm{Re}^{5/8}$ where the left limit is the Navier-Stokes region and the right limit is the triple-deck (see Figure 1). Realistic condensed layers are closest to the triple-deck, and an examination of the most general triple-deck solutions reveals that the interfacial waves may be considered in isolation from Tollmien-Schlichting instabilities in the air. The condensed layer is found to give accurate solutions providing that the water film is sufficiently thin on triple-deck scales. In cases where the film approaches finite thickness on triple-deck scales, it is found that Tollmien-Schlichting instabilities are still largely unaffected by the water film and that the condensed layer and other approximate solutions can predict qualitative trends of the interfacial instability, but that the full triple-deck is needed in order to obtain quantitatively accurate solutions. It should be noted that the linear-wave structure of the triple-deck is much richer than the condensed layer and admits a variety of instabilities that are not encountered when using the condensed-layer equations. In situations that are applicable to aircraft icing, a new simplified form of the triple-deck has been presented which reflects the large differences in air and water densities and viscosities.

Acknowledgements

This research was partially supported by the Icing Branch at the NASA Glenn Research Center under contract NAG3-2571 and by EPSRC Grant GR/N37551/01, Mathematical Theory of Internal Icing. The authors would like to thank Dr T. Bond, Dr M. Potapczuk and Dr J. Tsao for their helpful directions and suggestions during the course of this research.

References

1. R.W. Gent, N.P. Dart, and J.T. Cansdale, Aircraft icing. *Phil. Trans. R. Soc. London* A358 (2000) 2873–2911.
2. B.L. Messinger, Equilibrium temperature of an unheated icing surface as a function of air-speed. *J. Aeronaut. Sci*. 20 (1953) 29–42.
3. T.G. Myers, Extension to the Messinger model for aircraft icing. *AIAA Journal* 39 (2001) 211–218.
4. W. Olsen and E. Walker, Experimental evidence for modifying the current physical model for ice accretion on aircraft structures. *NASA (National Aeronautics and Space Administration) Technical Memorandum* 87184 (1987) 45pp.
5. S.N. Timoshin, Instability in a high-Reynolds-number boundary layer on a film-coated wall. *J. Fluid Mech.* 353 (1997) 163–195.
6. J.C. Tsao, A.P. Rothmayer and A.I. Ruban, Stability of air flow past thin liquid films on airfoils. *Comp. Fluids* 26 (1997) 427–452.
7. R.I. Bowles, P. Caporn and S.N. Timoshin, Nonlinear shortwave Tollmien-Schlichting instability in a boundary layer on a film-coated wall. *Proc. R. Soc. London* A454 (1998) 3223–3256.
8. S.N. Timoshin and A.P. Hooper, Mode coalescence in a two-fluid boundary-layer stability problem. *Phys. Fluids* 12 (2000) 1969–1978.
9. N.A. Pelekasis and J .A. Tsamopoulos, Linear stability of a gas boundary layer flowing past a thin liquid film over a flat plate. *J. Fluid Mech.* 436 (2001) 321–352.
10. A.P. Rothmayer and J.C. Tsao, Water film runback on an airfoil surface. AIAA Paper 2000–0237 presented at the AIAA 38th Aerospace Sciences Meeting (2000), available through *American Institute of Aeronautics and Astronautics* (http://www.aiaa.org).
11. S. Ozgen, G. Degrez and G.S.R. Sarma, Two-fluid boundary layer stability. *Phys. Fluids* 10 (1998) 2746–2757.
12. V.V. Bogolepov and V.Ya. Neiland, Viscous gas motion near small irregularities on a rigid body surface in supersonic flow. *Trans TsAGI* 1363 (1971).
13. V.V. Bogolepov and V.Ya. Neiland, Investigation of local perturbations in viscous supersonic flows. *Aeromechanics Collected Articles* Moscow Science pp. 104–118. (in Russian *Aeromekhanika. Sb. statej. Moskva. Nauka.* (1976) 104–118.). Translated in *Soviet Research-Fluid Mechanics Soviet Research/Scripta Technica* USA 2 (1980) 84–95.
14. F.T. Smith, P.W.M. Brighton, P.S. Jackson and J.C.R. Hunt, On boundary-layer flow past two-dimensional obstacles. *J. Fluid Mech.* 113 (1981) 123–152.
15. A.P. Rothmayer and F.T. Smith, Incompressible triple-deck theory. Part III Chapter 23 In: R.W. Johnson (ed.), *Handbook of Fluid Dynamics* Boca Raton: CRC Press (1998) pp. 23/1–23/24.
16. F.T. Smith, Laminar flow over a small hump on a flat plate. *J. Fluid Mech.* 57 (1972) 803–824.
17. B.D. Matheis, *Numerical simulation of thin air driven films.* M.S. Thesis Iowa State University Ames Iowa (2001) 49pp.